Scientific Research Publishing

Materials Sciences and Applications, 2026, 17(7), 149-168
https://www.scirp.org/journal/msa
ISSN Online: 2153-1188
ISSN Print: 2153-117X

Polycaprolactone and Poly(Lactic Acid) Filled with Low Content of Oxidized Carbon Nanotubes-Hydroxyapatite (o-CNT-HAp) Hybrid Filler: Effect of Proportion between o-CNT/HAp and Type of Polymer on the Properties and Interaction

Isabella Carneiro Gonçalves, Kaio Alves Brayner, Enzo Erbisti Garcia, Gerson Alberto Valencia Albitres, Luis Claudio Mendes

Instituto de Macromoléculas Professora Eloisa Mano, Universidade Federal do Rio de Janeiro, Centro de Tecnologia, Bloco J, Rio de Janeiro, Brazil
Email: isabellacg@ima.ufrj.br

How to cite this paper: Gonçalves, I.C., Brayner, K.A., Garcia, E.E., Albitres, G.A.V. and Mendes, L.C. (2026) Polycaprolactone and Poly(Lactic Acid) Filled with Low Content of Oxidized Carbon Nanotubes-Hydroxyapatite (o-CNT-HAp) Hybrid Filler: Effect of Proportion between o-CNT/HAp and Type of Polymer on the Properties and Interaction. *Materials Sciences and Applications*, **17**, 149-168.
https://doi.org/10.4236/msa.2026.177011

Received: May 26, 2026
Accepted: July 21, 2026
Published: July 24, 2026

Abstract

Multiwall carbon nanotubes are known as multifunctional materials due to their nanometric nature and specific physical and chemical properties. Their oxidation induces structural chemical modification leading to better interaction with polymers. In this context, it was studied the effect of low content (0.05 wt.%) of hybrid filler constituted of oxidized carbon nanotubes (o-CNT)/hydroxyapatite (HAp) at different proportions added to the sustainable polyesters-polycaprolactone (PCL) and poly(lactic acid) (PLA). Properties and polymer-filler interaction were assessed. By spin-spin relaxation times, T_1 showed no expressive variation for PCL and composites while spin-lattice relaxation times revealed that T_2 changed for PLA-o-CNT-HAp(2:1). Thermogravimetry showed that there was no significant alteration in thermal stability of PCL and composites but PLA-o-CNT-HAp(2:1) revealed a slight increase in thermal stability. Only PLA-o-CNT-HAp(2:1) exhibited increase of crystalline melting temperature and decrease of degree of crystallinity whereas no change was achieved for PCL composites. Owing to the low content of fillers, the rheological measurement was driven by polymer matrices. The results suggested that the chemical structure of polymer matrix and the arrangement of

the hybrid fillers jointly or to some extent influenced the chemical interaction and properties of the composites.

Keywords

Polycaprolactone, Poly(lactic Acid), Oxidized Carbon Nanotubes, Hydroxyapatite, Composite

1. Introduction

Polycaprolactone (PCL) and poly(lactic acid) (PLA) are among the most important and extensively used as biodegradable polymer. They possess highlighted features such as biocompatibility, mechanical properties, processability, slow degradation rate and so on. Although both are biodegradable, each one has different origins, namely PCL comes from fossil source and PLA from renewable sources by fermentation of corn starch, sugarcane to generate lactic acid which after its polymerization produces PLA [1] [2]. Recognized as biodegradable, biocompatible, and environmentally friendly polymers, PCL and PLA found applications in various sectors of human activity, notably in the biomedical one. Both present some shortcomings which are surpassed by incorporation of fillers for reinforcing or with specific features such as silica, oxidized carbon nanotubes, graphene, hydroxyapatite, carbon nanotubes and so on [3]-[9]. Single and multiwall carbon nanotubes and its oxidized forms have been added to different polymer matrices at low content. Dave *et al.* synthesized a hydrogel with gum ghatti as biopolymer (GG), acrylic acid (AA), ammonium persulphate as initiator, and methylene bisacrylamide (MBA) as cross-linker and 0.01 - 0.05 (wt.%) oxidized multiwalled carbon nanotubes (-o-MWCNT). The authors reported that the increase of -o-MWCNT amount rendered consistent crosslinking, improving the network connections besides the storage modulus and complex viscosity [10]. Carbon nanotubes were treated by mixing sulfuric acid and nitric acid at different times (15 to 120 minutes) by Lavagna *et al.* It was added (0.1 wt.%) to cement-based composites and its effect on properties was evaluated. It was observed that for sample treated at 90 minutes, it was obtained cement-based composites with a gain in flexural strength, fracture energy and compressive strength [11]. Kim *et al.* prepared composites based on epoxy resin and oxidized carbon nanotubes (0.005 to 3 wt.%), oxidizing procedure involving the use of nitric acid in different concentration and time, at 100˚C. The authors highlighted that rigorous conditions of oxidation related to high acid concentration and temperature damage its structure impacting its electrical properties [12]. Zhou *et al.* developed a scaffold based on PCL with silver nanoparticles (AgNP). It was concluded that AgNP provided effective antibacterial activity besides promoted osteogenic cell functions addressing its application for bone regeneration [13]. Composites of PCL with phosphocalcified oxidized carbon nanotubes were prepared by Jolfaei and Haddadi-Asl

searching use as osteogenic promoter. The authors highlighted the simultaneous optimization with respect to pore structure, surface chemistry, and ion-release capability [14]. The effects of hydroxyapatite (HAp) and chamomile extract (CE) on composites based on blend of PCL and poly(ethylene oxide) (PEO) were studied by Fallah *et al.* It was reported that the incorporation of HAp (1% w/v) improved mechanical and thermal features while CE upgraded the biological performance [15]. Jiang *et al.* developed a bilayered sponge dressing based on PLA incorporated with hybrid filler of oxidized carbon nanotubes-quaternized carboxymethyl chitosan (QCMCS@GO). The authors reported that GO provided reinforcement, modified chitosan promoted platelet activation and intrinsic coagulation pathway while PLA acted as physical barrier mainly against *Staphylococcus aureus* and *Escherichia coli* [16]. Pandey *et al.* prepared membrane for oil/water separation having PLA as based-polymer incorporating a hybrid filler of cross-linked quaternary ammonium oxidized carbon nanotubes (CSQAGO). With 6 wt.% of CSQAGO, the membrane revealed high efficiency of separation besides notable colony inhibition against *Escherichia coli* [7]. Graphene nanofiller (0.075 wt.%) was added to polymers mixing namely epoxy, PCL and poly(glycol ethylene) searching improvement as coating for corrosion protection and self-healing of metallic surface. Its incorporation provided better tensile strength, healing efficiency and anticorrosive performance [17]. Litha *et al.* investigated the biomechanical properties of the composites based on polymer blend PLA/PCL (70/30) embedded with hybrid filler of oxidized carbon nanotubes/hydroxyapatite (GO/HA, 0.04/15 wt./wt.%). The authors highlighted improvement of tensile strength and Young's modulus besides microbial activity against *Staphylococcus aureus and Pseudomonas aeruginosa* [18]. Pekdemir *et al.* investigated the effects of multiwalled carbon nanotube (MWCNT, 0.1, 0.2, 0.5 and 1.0 wt.%) on the blend's PCL/poly(vinyl chloride) (PCL/PVC). The authors depicted that the ultimate stress, resilience and toughness of the composite decreased linearly with amount of MWCNT [19]. Titanium oxide (TiO_2) was added to blends of PLA with poly(hydroxyalkanoate) (PLA/PHA). It was revealed the decrease of blend's glass transition temperature, reduction in elasticity and a progressive increase of stiffness with filler content [20]. Thermal degradation and shape memory recovery of PCL/PVC at variable proportions were studied by Demir. Shape memory recovery test revealed that the PCL/PVC (70/30) exhibited great strain recovery [21]. PCL/poly(methyl methacrylate) (PCL/PMMA, 80/20 wt./wt.%) was filled with MWCNT (0.01; 0.03; 0.06 wt.%). With the increase in MWCT content, glass transition temperature diminished while melting temperature and mechanical properties increased [22]. PCL matrix was filled with oxidized carbon nanotubes (GO), reduced oxidized carbon nanotubes (rGO), multilayered graphene (Gmec) and low-oxidized graphene (Ganodic). PCL/rGO and PCL/GO membranes presented the highest biomolecule markers for astrocyte (support cells) differentiation [23]. This work focused mainly the evaluation of composites based on PCL and PLA with hybrid fillers of oxidized carbon nanotubes (o-CNT)/hydroxyapatite (HAp) at low content (0.05 wt.%).

The effect of polymer structure and filler constitution were considered for assessing physico-chemical properties and polymer-filler interaction.

2. Experimental

Multilayer carbon nanotubes (MWCNT) (98% purity), hydroxyapatite (90% purity), polycaprolactone (M_n = 45,000), poly(lactic acid) (1.24 g/cm^3), sulfuric acid and nitric acid were purchased and used as received.

2.1. Chemical Modification of Multilayer Carbon Nanotubes (MWCNT)

The chemical modification of multilayer carbon nanotubes has already been described previously [24]. Herein, a brief description. 2 g of MWCNT was added to 400 mL of sulfonitric solution H_2SO_4/HNO_3 (3:1). The dispersion was kept under stirring and refluxing, at 110˚C, for 3 hours. After that, the medium was diluted (four times) by distilled water accommodated in dialysis membranes and immersed in distilled water until reaching pH 6.0. At the end, the content was conducted to evaporate until constant weight. The black powder was labeled as oxidized-CNT (o-CNT).

2.2. Synthesis of Hybrid Fillers

Hybrid fillers of o-CNT and hydroxyapatite (HAp) were prepared through acetone dispersion, at different proportions. The first one consisted of blending by handling o-CNT-HAp (1:2) and the second one of o-CNT-HAp (2:1). These proportions were thought in order to assess how its constitution impact on the physico-chemistry properties of the composites. For both, the HAp dispersion was dripped slowly to the o-CNT dispersion, at 25˚C, under magnetic stirring, for 24 hours. After that, the content was submitted to evaporation and a dark brown powder was attained being labelled o-CNT-HAp(1:2) and o-CNT-HAp(2:1), respectively.

2.3. Composites Preparation

PCL and composite films were obtained by its dissolution in methylene chloride (10%, m/v) following the addition of each filler MWCNT, o-CNT, HAp and o-CNT-HAp(1:2) (0.05 wt.%), maintaining under stirring for 24 h. After that, the dispersion was poured onto Petri dish, kept for complete solvent evaporation to attain a film. For comparison, a film of PLA and PLA plus o-CNT-HAp(2:1) (0.05 wt.%) was prepared as mentioned above. Summarizing, the samples were labeled as follows: PCL, PCL-MWCNT, PCL-o-CNT, PCL-HAp and PCL-o-CNT-HAp(1:2); PLA and PLA-o-CNT-HAp(2:1). In all cases, the low content of filler was thought to be enough to attain better dispersion and promote changes in physico-chemical properties of the polymer matrix.

2.4. Infrared Spectroscopy

Fourier-transform infrared spectroscopy (FTIR) was performed using a Perkin

Elmer Frontier equipment in the of 4000 - 400 cm^{-1}, with 120 scans and a resolution of 4 cm^{-1}.

2.5. X-Ray Diffraction

The crystallographic structure was evaluated using a wide-angle X-ray diffractometer Rigaku Miniflex, employing CuKα radiation with a wavelength λ = 1.5418 Å, a Ni filter, a current of 20 mA, a voltage of 20 kV, 2θ between 2˚ - 50˚ and resolution of 0.05˚.

2.6. Time-Domain Nuclear Magnetic Resonance (TD-NMR)

Molecular relaxation of PCL and composites was performed through spin-spin relaxation, transverse relaxation time (T_2), by magic sandwich echo-free induction decay (MSE-FID) by using time domain nuclear magnetic resonance on a MARAN Ultra 0.54 T (23.4 MHz for 1H) equipment, with a probe diameter of 18 mm and WinFit 2.4-point adjustment software. The analysis was performed at temperature of 30˚C ± 2˚C, with a 2-Eco-Solid pulse sequence, a pulse duration of 90˚ in 7.5 μs, with 2048 points spaced 0.5 μs apart. The number of accumulations corresponds to 64, with a recycling time of 1 second and a receiver gain of 8%. The adjustment function for the MSE-FID signals was determined by Equation (1): A_R, amplitude or fraction of the rigid region; A_M, amplitude or fraction of the moving region; T_2*, transverse relaxation time of each of the fractions obtained by the equipment; μ_b, centroid of the Gaussian function; K, offset or baseline of the relaxation signal that compensates for the influence of noise during nonlinear tuning. The signal is governed by two components. The first (on the left) is related to highly rigid ^{1}H nuclei and is governed by a Gaussian function. The second (on the right) is characterized by more mobile hydrogens that exhibit higher T_2H values and an exponential decay according Neto *et al.* [25]. The fraction of each domain rigid domain (A_R) and mobile domain (A_M) was calculated according to Equation (2). T_2 relaxation analysis was selected for PCL and its respective composites since better resolution was achieved.

$$A(t) = A_R \exp\left[-\left(\frac{\tau-\mu_b}{2T_{2+R}}\right)^2\right] + A_M \exp\left[-\left(\frac{\tau}{T_{2+M}}\right)\right] + K \quad (1)$$

$$X(\%) = \frac{A^x}{(A_R + A_M)} \times 100 \quad (2)$$

Molecular motion of PLA and composite was performed in the equipment described above evaluating the longitudinal relaxation time (T_1), also known as spin-lattice relaxation, which result of the existence of transient magnetic moments produced by the rotational and translational movements of neighboring molecules [25] [26]. Two replicates were evaluated.

2.7. Thermogravimetry

Samples thermal stability was conducted in a TA Instruments Q-500 equipment,

in the range of 30˚C - 700˚C, at 10˚C/min, in a nitrogen atmosphere. T_{onset}, T_{10}, T_{max} and residue were evaluated.

2.8. Differential Scanning Calorimetry

Differential scanning calorimetry was performed using a TA Instrument Q1000. Five thermal cycles were performed according to ASTM D3418. In the first cycle, the sample was heated from −80˚C to 200˚C at 10˚C/min, using nitrogen as the carrier gas, and held at this temperature for 2 minutes to eliminate the thermal history. A cooling cycle was then performed to −80˚C at the maximum speed of the equipment. A second heating cycle was performed under the same conditions as the first. In the fourth cycle, a second cooling cycle was performed from 200 to −80˚C at 10˚C/min, where it was possible to determine the cooling crystallization temperature (T_c). The fifth cycle was conducted under the same conditions as the first, and the crystalline melting temperature (T_m) was registered. Degree of crystallinity was calculated based on Equation (3) where ΔH_m, experimental enthalpy of fusion and ΔH_m^0, the enthalpy of fusion of 100% crystalline PCL, 139.5 J/g [27] and PLA 93.6 J/g [28], Φ corresponds to the content of the added particle.

$$X_c = \left[\frac{\Delta H_m}{\Delta H_m^0 (1-\Phi)}\right] \times 100 \quad (3)$$

2.9. Rheology

Rheology evaluation was conducted by using a TA rheometer, model AR-2000, 25 mm in diameter with parallel plate geometry at 60˚C. The procedure was performed in an inert atmosphere under dynamic conditions. In order to observe the linear viscoelasticity region of the films, deformation tests were performed at a frequency of 1 Hz. Storage and loss moduli, as well as complex viscosity, were also determined. Two replicates were evaluated.

3. Results and Discussion

3.1. Fourier Transform Infrared Spectroscopy (FTIR)

Figure 1 shows samples' spectra. PCL showed absorptions at 2950 cm^{-1} (asymmetric stretching of CH_2), 2865 cm^{-1} (symmetric stretching of CH2), 1730 cm^{-1} (symmetric stretching of C=O), 1294 cm^{-1} (stretching of C-O and C-C in the crystalline phase), 1234 and 1167 cm^{-1} (symmetric and asymmetric stretching of C-O-C), 1106 and 1049 cm^{-1} (O-C vibrations) in agreement with reported by Adeniyi *et al.* [29]. PLA absorptions were ester carbonyl (C=O) stretching at 1750 cm^{-1}, C–H bending modes at 1450 and 1340 cm^{-1}, and the C–O–C stretching vibrations in the region between 1260 and 1050 cm^{-1} which are in accordance to published by Justino Netto *et al.* [30]. To guide the evaluation of the hybrid fillers, spectra of them and their precursors are described. HAp absorptions were found at 650, 1631 and 3435 cm^{-1} (hydroxy group), 1037 and 1095 cm^{-1} (phosphate crystalline arrangement) and 560, 601 and 961 cm^{-1} (phosphate group) which were

endorsed by several authors [31]-[33]. For o-CNT, multi absorptions were detected namely intense and enlarged peak at 3495 cm^{-1} (hydroxy group), 1725 cm^{-1} (carbonyl stretching), 1624 and 1497 cm^{-1} (C=C ring stretching), 1435 and 995 cm^{-1} (C-O-H, in plane and out of plane respectively), 1232 cm^{-1} (C-C-O stretching), 1139 and 1067 cm^{-1}, vibrations of O=S=O(OH), 889 and 846 cm^{-1} (C-H aromatic ring vibrations) following what was published by Puliyasseri *et al.* and Saipanya *et al.* [34] [35]. The spectrum of each hybrid filler shows fidelity to the proportions of HAp and o-CNT. For o-CNT-HAp(1:2), 3416, 2973, 2930, 2859, 1740, 1622, 1095, 1037, 964, 865, 634, 605 and 564 cm^{-1} were highlighted. For o-CNT-HAp(2:1), absorptions 3602, 3552, 2975, 2923, 2852, 1740, 1621, 1420, 1150, 1093, 1013, 958, 657, 599 and 567 cm^{-1} were registered. With respect to the PCL-o-CNT-HAp(1:2) and PLA-o-CNT-HAp(2:1) composites their spectra display the predominant absorptions of polymer-base which could be associated with the hiding of fillers' absorptions.

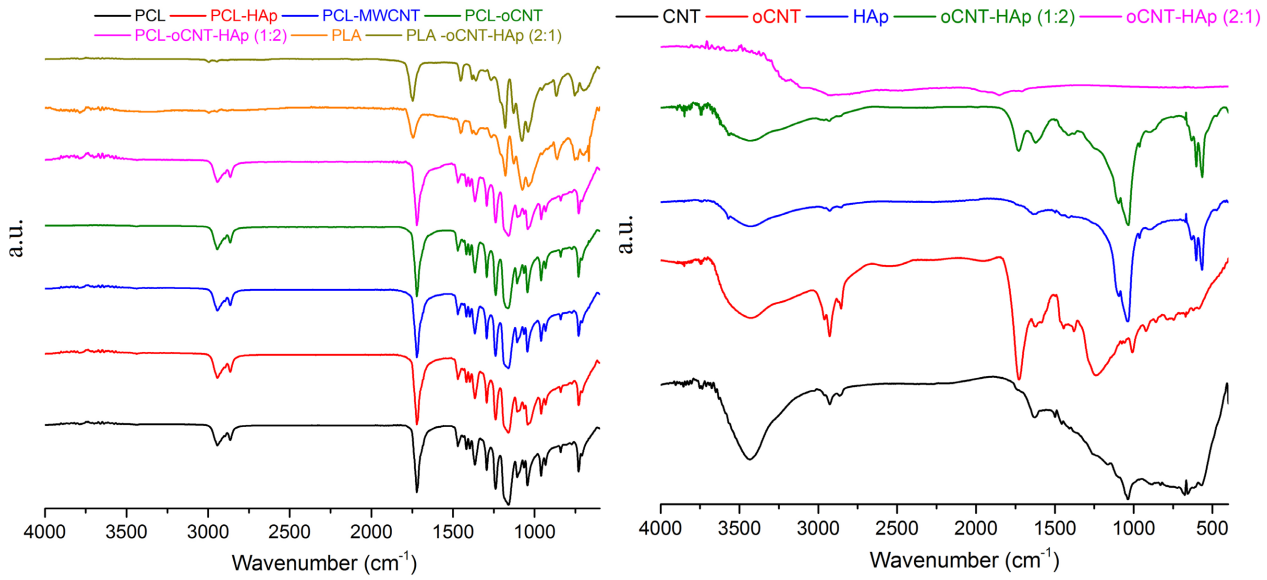

Figure 1. Infrared spectra of fillers and composites.

3.2. Wide-Angle X-Ray Diffractometry

Figure 2 presents the samples' diffraction patterns. PCL exhibits two diffraction angles (2θ) at 21.5 (110) and 23.8˚ (200) endorsed by publication of Doostmohammadi *et al.* [36]. PLA displays diffraction angle at 16 - 17 representing its α-crystalline form as reported by Tamburini *et al.* [37]. HAp presented diffraction angles at 25.9˚ (201), 26.5˚ (002), 30.2˚ (211), 31.9˚ (112), 33.0˚ (300), 34.2˚ (202), 40.0˚ (410), 46.9˚ (222) and 49.6˚ (213) finding correspondence with the results reported by Targońska *et al.*, Cao *et al.* and Nurbaiti *et al.* [32] [33] [38]. Before commenting the o-CNT diffraction patterns, it is necessary to emphasize that MWCNT precursor presented diffraction angles at 25.9˚ (002) and 43.1˚ (100) being the first one associated with its concentric graphite structure. Interesting to note that o-CNT revealed the first 2θ angle displaced to 23.5˚ showing variation

of $d_{spacing}$ from 3.44 to 3.77 nm. This increase in interplanar spacing is indicative of the size and structure of the crystals, justified by the presence of hydroxyls, carbonyls, and sulfonic groups possibly adhered to the surface of the o-CNT, after the chemical modification of MWCNT [39]. PCL-o-CNT-HAp(1:2) exhibits 2θ angle at 21.3, 21.9 and 22.6˚ related to PCL besides 23.6˚ which could be overlapping of 2θ of PCL and o-CNT; a low intense 2θ around 30˚ could be attributed to HAp apatite crystalline plane. Irani *et al.* developed scaffold by co-electrospun of PCL, gelatin, chitosan and carbon nanotubes (CNT, 0.1, 0.2 and 0.4 wt.%) for tissue engineering. X-ray diffraction evaluation did not detect CNT-related 2θ angles which were associated to its low concentration [40]. PLA-o-CNT-HAp(2:1) shows diffraction pattern similar to PLA alone which could be attributed to the low filler content.

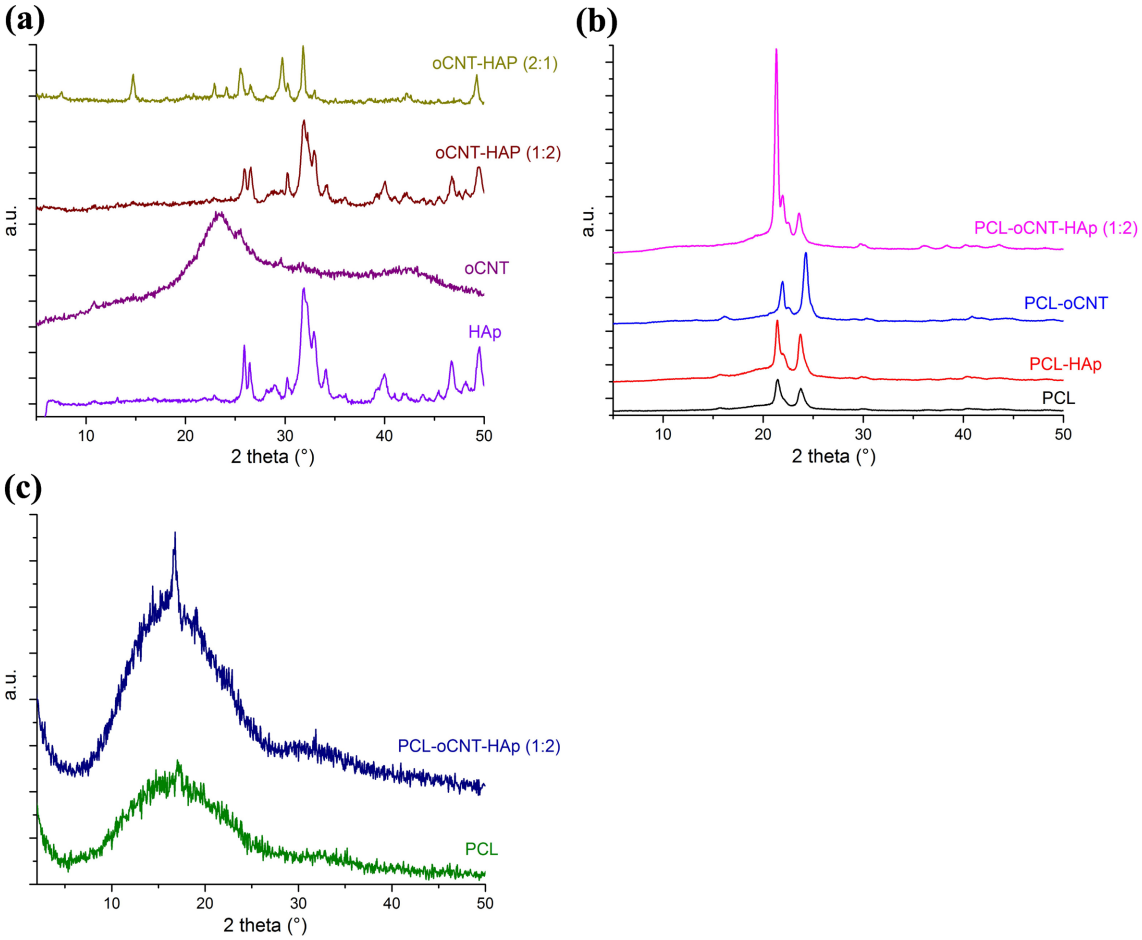

Figure 2. DRX patterns of fillers and composites.

3.3. Time-Domain Nuclear Magnetic Resonance

The application of magnetic field in the study of molecular motions is considered a powerful technique to evaluate relaxation times. Different nuclear magnetic resonance processes named longitudinal and transverse relaxation times allow to access the molecular mobility of polymer, fluid and so on. Herein, longitudinal magnetization (T_1) and transverse magnetization (T_2) were applied to evaluate the ef-

fect of fillers on the polymer molecular motion. Table 1 presents data (T_2 and % of area) of transverse magnetization of PCL and composites. In general, for all composites, T_2 increased when faced up to PCL alone indicating increase of molecular mobility. When it compares the percentage of rigid and mobile domains it was noticed that were invariable. Only the PCL-o-CNT composite got away from that trend. Although T_1 is determined by distinct physical process when compared to T_2 it is also valid for evaluation of polymer relaxation. T_1 was applied to assess the relaxation mode of PLA and PLA-o-CNT-HAp(2:1). Figure 3 presents the domain curves of PLA and composite. Both showed relaxation curves with two domains: flexible (shorter relaxation time) and rigid (longer relaxation time). At relaxation times below 100.000 ms, the domain was related to the mobility of the amorphous phase chain; the second, more intense peak, in the region of 100,000 - 2500.000 ms, was related to the conformation of more rigid, packed chains, or those with greater mobility hindrance. The influence of o-CNT-HAp(2:1) on the molecular mobility of the PLA phases was sharply evidenced by the enlargement of the domain curves and their shift to lower and higher values along the time axis. The lowering of T_1 indicates higher chain mobility while on the contrary its increase reveals lower chain mobility. Catauro *et al.* synthesized nanocomposites of SiO_2 with PCL (0, 6, 12, 24 and 50 wt.%) by sol-gel process. The occurrence of H-bonds among carbonyl groups of PLA chain and Si-OH was evaluated by infrared spectroscopy (FTIR) and solid-state nuclear magnetic resonance (NMR). By ^{13}C-CPMAS-NMR (cross-polarization magic-angle spinning nuclear magnetic resonance), two resonance peaks were detected which were associated to the PCL crystalline and amorphous phases. Still, ^{1}H and ^{13}C-CPMAS-NMR applied to SiO_2/PCL composites revealed enlargement of carbonyl peak with the increase of PCL content which it was considered as non-covalent interaction among PCL oxygens and the -OH moieties of silicon dioxide [41]. Through molecular dynamics simulations, Çelik *et al.* intended to find a guide for design and optimization of molecular-level interaction of polymer-nanoparticle in composites of poly(lactic-co-glycolic acid) (PLGA) and poly(ε-caprolactone) (PCL) with oxidized carbon nanotubes (GO) and reduced oxidized carbon nanotubes (rGO). A series of evaluations such as hydrogen bond occupancy, radius of gyration, potential and binding energies, radial distribution functions, and solvation free energy were experienced. The authors found that 75:25 PLGA-GO and 75:25 PLGA-rGO were the most stable interaction profiles among PLGA variants, while PCL-GO was the most stable [42]. In our study, both polymers are biodegradable polyesters in which carbonyl groups could form hydrogen bonds with reactive groups onto o-CNT. In the case of PCL-o-CNT-HAp(1:2), this type of interactions was avoided or in lower extent owing to the lower availability of the reactive groups. In Table 1, when o-CNT is added to PCL, there is great variation on T_2 and domain percentage of the polymer. The addition of HAp to PCL produces no changes on the PCL relaxation parameters. The incorporation of o-CNT-HAp(1:2) (0.5%) causes a negligible change in T_2 and none in the domain percentages which could indicate that in the o-CNT-HAp(1:2) there is low availability of the carbonyl and hy-

droxyl groups of o-CNT leading to lower level of polymer-filler interaction in the PCL-o-CNT-HAp(1:2) composite. The spatial degree of freedom of the methylene and chains entanglement of the PCL could be additional factors to affect polymer-filler interaction considering the availability of oxygen atoms to form hydrogen bond with carbonyl and hydroxyl groups in o-CNT. On the contrary, for PLA-o-CNT-HAp(2:1), in the repeat unit of PLA only a secondary carbon linked as follows –H-C-CH_3 appeared between two ester groups resulting in no variation on the degree of freedom. If compared to PCL, even tangled the PLA chains favor the formation of hydrogen bond between the oxygen atoms of the ester groups, near to each other, and carbonyl and hydroxyl groups in o-CNT. This could endorse the more effective action of o-CNT-HAp(2:1) on the PLA relaxation process. As a suggestion, Figure 4 shows step-by-step the structural constitution of the fillers. o-CNT possesses several carbonyl groups of carboxyl acid/ketone and hydroxyl groups onto its surface while HAp owning two hydroxyl anion for charge equilibrium. When o-CNT and HAp are physically mixed at 1:2 proportion most reactive groups onto o-CNT are hidden. On the contrary, at 2:1, o-CNT most reactive groups are available. Then, when mixed, the pair PLA and o-CNT-HAp(2:1) greater possibility of chemical interaction arises while on the contrary in the pair PCL and o-CNT-HAp(1:2) is more difficult.

Table 1. T_2 relaxation time of PCL and composites.

Samples	T_{2rigid}/Area (ms/%)	$T_{2mobile}$ /Area (ms/%)
PCL	7.12/57	172/43
PCL-CNT	7.37/58	187/42
PCL-o-CNT	6.90/74	212/26
PCL-HAp	7.28/57	176/43
PCL-o-CNT-HAp(1:2)	8.28/59	182/41

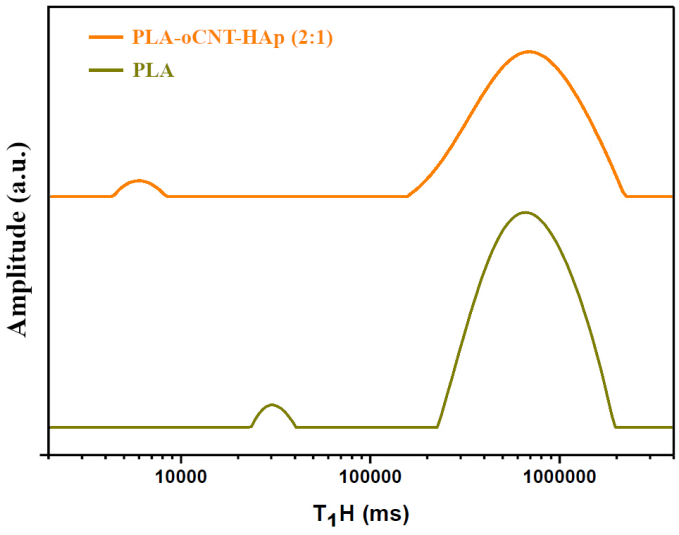

Figure 3. T_1 relaxation domain curves of PLA and PLA-o-CNT-HAp(2:1).

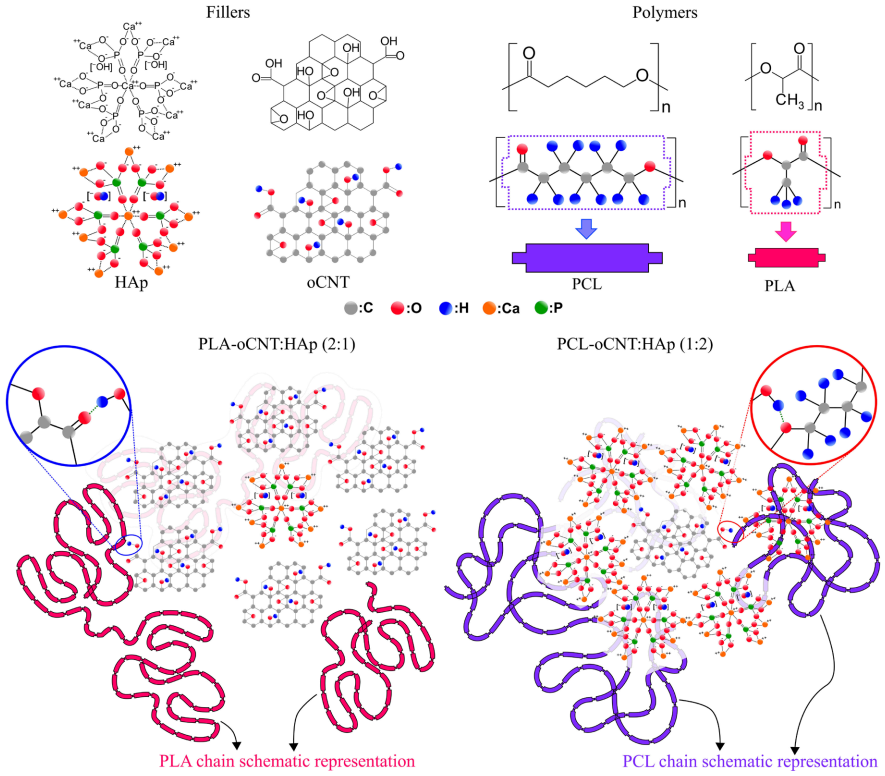

Figure 4. Fillers structural constitution: speculative schematic representation.

3.4. Thermogravimetric Analysis

Figure 5 exhibits the loss mass and derivative curves. Either PCL and composites or PLA and PLA-oCNT-HAp(2:1) presented only one stage of mass loss. Except for PLA-oCNT-HAp(2:1), for the others samples a unique derivative peak was noticed. Table 1 displays the thermogravimetric data. For all fillers tested, PCL composites revealed decrease on T_{onset}, T_{10} and T_{max}. Inversely, the presence of oCNT-HAp(2:1) into PLA matrix denotes increase on T_{onset}, T_{10} and T_{max}. Fillers can play a role in increasing or decreasing polymer matrix thermal stability in polymeric composites. Mohammed *et al.* (2025) studied the incorporation of silica (0 - 40 wt.%) on the properties of polycaprolactone/poly(vinyl chloride) (PCL/PVC). The authors registered multi-step decomposition and deduced that silica residue improved the thermal stability at high temperatures [43]. Poljacek *et al.* evaluated the action of PCL and nanosilica when incorporated in PLA. The addition of 1 and 3 wt.% of nanosilica in PLA did not alter its thermal while for PLA/PCL blends an increase of thermal stability was noticed [44]. Espirito Santo *et al.* investigated the influence of biosilica (extracted from Dragmacidon reticulatum) at different proportions (10, 15 and 20 wt.%) on PCL samples from electrospun fibers and casting films. For all composites, the thermal decomposition occurred at lower temperatures which denoted decrease of thermal stability [3]. Taha *et al.* reported a study on hybrid composites of PLA filled with zinc oxide (ZnO) nanoparticles and varied content of oxidized carbon nanotubes (GO) (3, 4 and 6 wt.%). Significant enhancement of thermal stability was observed at high content of GO which was attributed

to the filler network which effectively hindered the release of volatile degradation matters [45]. **Table 2** displays the thermogravimetric data of the PCL and PLA materials. For PCL-based composites, T_{onset}, T_{10} and T_{max} showed a tendency to decrease but the decrement was more evidenced for the PCL-oCNT-HAp(1:2) which could be imputed to some filler catalytic action. Reversely, for PLA-oCNT-HAp(2:1), T_{onset}, T_{10} and T_{max} were significantly higher denoting upper thermal stability which endorses the hypothesis of better chemical interactions between polymer matrix and filler. Summarizing, the thermogravimetric data can suggest that either polymer structure or filler composition had influence on the thermal stability of the composites. If compared PCL-oCNT-HAp(1:2) and PLA-oCNT-HAp(2:1) composites, in each one polymer matrix and filler had inverse action on their thermal stability. Herein, it was possible to infer that the composite PLA-oCNT-HAp(2:1) possesses high thermal stability which could be imputed to the occurrence of chemical interaction between constituents. On the contrary, thermal stability tends to decrease for all PCL composites probably owing to a gap of chemical interaction between polymer and fillers.

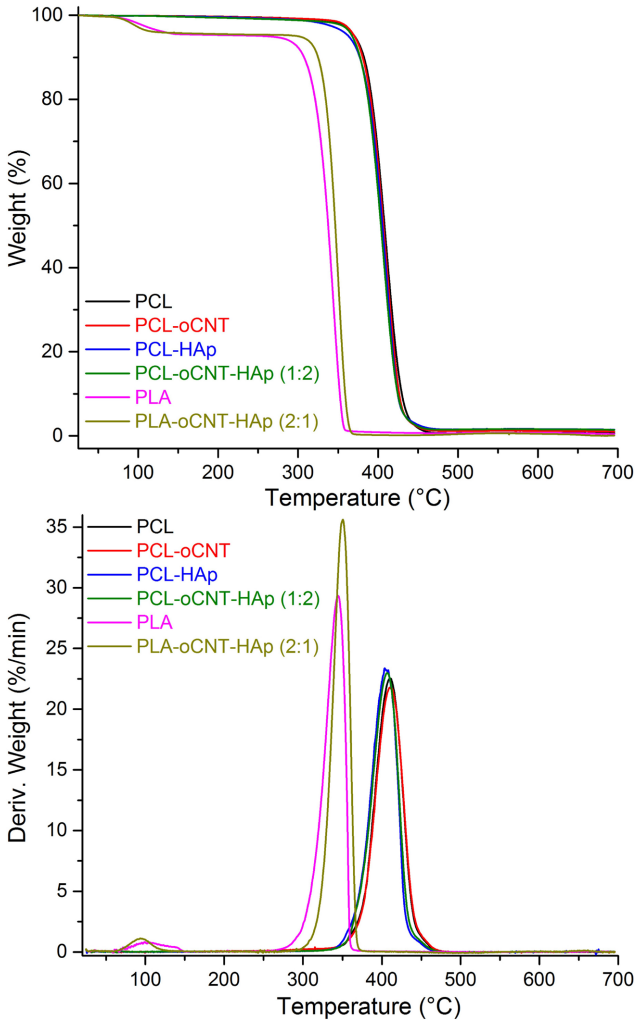

Figure 5. Mass loss and derivative curves of PCL and PLA materials.

Table 2. Thermogravimetric data of PCL and PLA materials.

Samples	T_{onset} (˚C)	T_{10} (˚C)	T_{max} (˚C)	Content of degradation (%)
PCL	386	382	411	99.4
PCL-HAp	385	381	408	99.0
PCL-oCNT	384	379	408	99.0
PCL-oCNT-HAp(1:2)	382	377	407	98.6
PLA	323	302	330	99.5
PLA-oCNT-HAp(2:1)	334	334	350	99.9

3.5. Differential Scanning Calorimetry

Figure 6 shows the third heating curves of PCL and PLA materials. For the third heating curves of PCL, it was detected the melting temperature (T_m). On the other hand, their counterpart for PLA materials showed T_g and T_m besides heating crystallization temperature (T_c). **Table 3** displays the calorimetric data of the PCL and PLA materials. With respect to PCL, its composites did not show significant variations on the calorimetric data. The values of T_c and T_m are in accordance with those reported by Mohammed *et al.* [43]. Similarly, for all composite, X_c was invariable. For PLA, T_g and T_m value are agreement with what was published by Oliver-Cuenca *et al.* [46]. In the same article, it is described that PLA homopolymer possesses four polymorphic structures named α, α', β, and γ. α-phase is the most common and stable crystalline structure. A'-phase can occur at lower crystallization temperatures. β-phase is formed by mechanic stress combining high temperature and high drawing ratio. γ-form is obtained through specific crystallization condition, epitaxial crystallization. Herein, none of the conditions mentioned for the appearance of polymorphism was applied, then the double T_m peaks were associated to the formation of crystals of different sizes. With respect to PLA crystallization temperature (T_c), its value was endorsed by the article of Akdevelioğlu *et al.* [28]. For PLA-oCNT-HAp (2:1), it was observed that the T_g and T_c of PLA were shifted to higher temperature, a unique melting temperature (T_m) was detected while the degree of crystallinity (X_c) diminished. The effects on the PLA calorimetric characteristics by addition of PCL (0 - 50 wt.%) and nanosilica (1 and 3 wt.%) were investigated by Poljacek *et al.* When alone, the incorporation of nanosilica in PLA promoted an increase of degree of crystallinity (X_c). In blend, with or without addition of nanosilica, for PLA, X_c did not show any tendency while X_c of PCL phase decreased when its content was 30 wt.%; above this amount X_c stabilized. With respect to the crystallization temperature (T_c) and melting temperature (T_m), both were invariable for PLA and PLA/PCL blends, with or without the presence of nanosilica [44]. Lomakin *et al.* studied composites of PLA with layered nanomodifiers-graphene nanoplates and sodic montmorillonite (0, 1, 5 and 10 wt.%). The calorimetric data revealed that T_g and T_m were practically invariable. Independent on the fillers amount, both ones showed increase on T_c and X_c which the authors associated to the role as nucleating agent promoting PLA crystallization [47]. Herein, it was evidenced that not only the amount of

filler but its chemical nature and constitution besides the polymer chemical structure address the interaction polymer-filler in polymer composite. In the case of PCL-o-CNT-HAp(1:2), no variation in calorimetric data could be imputed to the lack of interaction PCL with o-CNT-HAp(1:2) because of quasi total occlusion of the carbonyl and hydroxy groups in o-CNT by HAp hindrance. For PLA-o-CNT-HAp(2:1), the existence of hydrogen bond between carbonyl and hydroxyl groups in o-CNT and oxygen atoms in PLA chains favors the increase of T_c but create an obstacle to the diffusion of PLA chains to the crystallization centers decreasing the X_c. Summarizing, the DSC results emphasized that structural arrangement of the fillers o-CNT-HAp(1:2) and o-CNT-HAp(2:1) was the reason for the differences found in the calorimetric results. PLA and o-CNT-HAp(2:1) attained a certain degree of chemical interaction which is absent or in lower extent that found for PCL and o-CNT-HAp(1:2). TDNMR and TGA endorsed these findings.

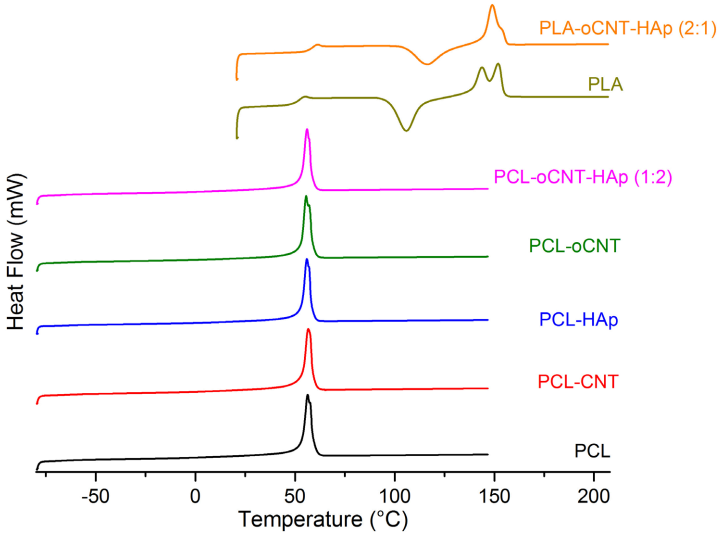

Figure 6. Precursors and composites heating curves (third cycle).

Table 3. Precursors and composites calorimetric data.

Samples	T_c (˚C)	T_m (˚C)	X_c (%)	T_g (˚C)
PCL	30	56	51	−63
PCL-HAp	29	56	52	−63
PCL-oCNT	30	56	51	−63
PCL-o-CNT-HAp(1:2)	32	56	51	−63
PLA	106	144/152	31	55
PLA-o-CNT-HAp(2:1)	117	149	26	62

3.6. Rheology

Figure 7 presents the moduli (storage and loss) and complex viscosity curves. For all samples, storage modulus (G') increased with frequency. The curve of PCL-CNT is separated from the others. The curves of PCL, PCL-o-CNT, PCL-HAp and PCL-o-CNT-HAp(1:2) are superimposed while the curves of PLA and PLA-o-

CNT-HAp(2:1) are also overlapped. For loss modulus (G"), the curves of PCL, PCL-CNT, PCL-HAp and PCL-o-CNT-HAp(1:2) are superimposed. The curves of PLA and PLA-o-CNT-HAp(2:1) are overlapped and laid out as intermediate related to the others. Immediately below, the curve of PCL-o-CNT can be seen. With respect to $|\eta^*|$, the curves of PLA and PLA-o-CNT-HAp(2:1) are upper than others being the latter with higher viscosity value. Following, the curves of PCL, PCL-CNT, PCL-HAp appeared practically superimposed while immediately below the curve of PCL-o-CNT is seen. In the range of frequency studied, PCL, PCL-CNT, PCL-HAp and PCL-o-CNT-HAp(1:2) behaved as a Newtonian fluid while PLA and PLA-o-CNT-HAp(2:1) resembled as pseudoplastic fluid. Table 4 displays the G', G" and G"/G' ratios of the samples at 10^1 and 10^2 rad/s. Either PCL and composites or PLA and composites the values of G' and G" reflected the response time of the materials. In this type of measurement, both increased at high frequency once polymer chains, microstructures, distribution and dispersion of fillers exerted influence on chain relaxation time and flowability. Herein, at high frequency, the chain relaxation time was not achieved and then the material response is rigidity. As the amount of filler was very low either in PCL or in PLA, the results in the rheological evaluation were driven mainly among neighboring polymers chains through restrict mobility to each other.

This explanation was validated by the values of ratio G"/G'.

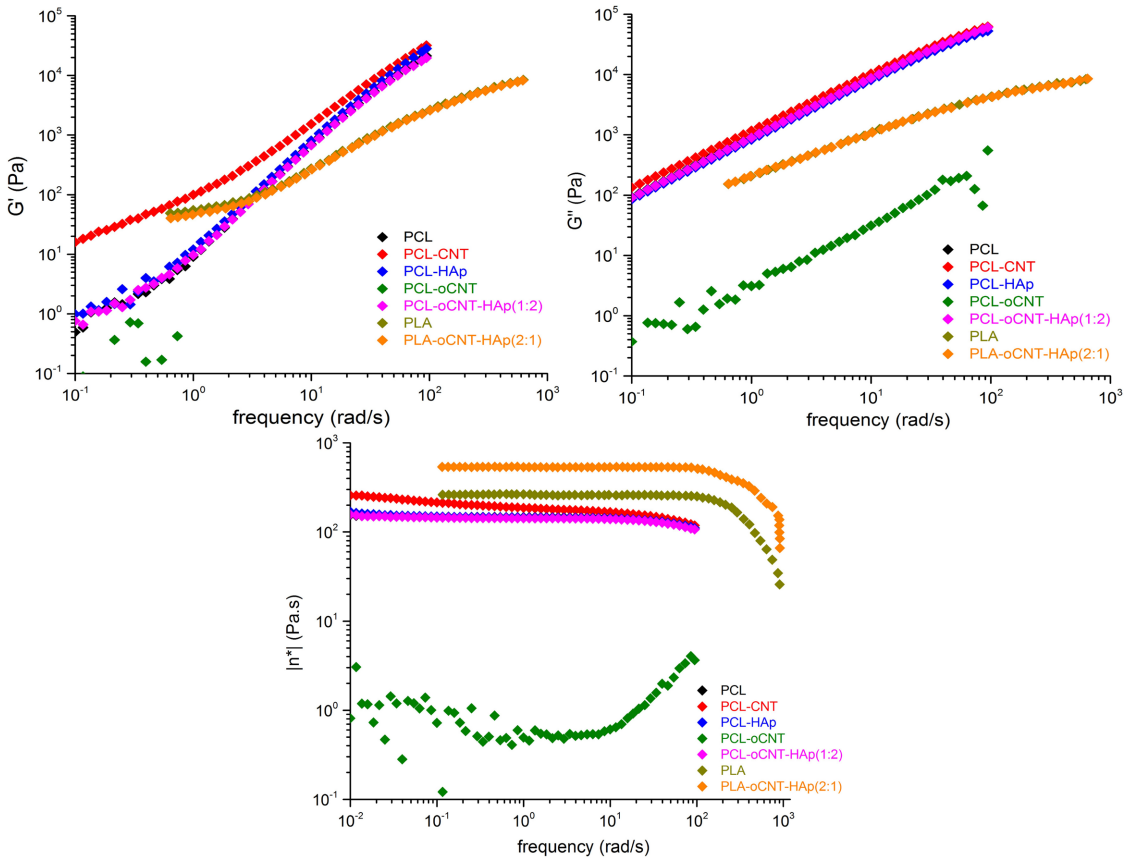

Figure 7. Precursors and composites moduli and complex viscosity curves.

Table 4. G', G" and G"/G ratio at different frequencies.

Sample	Frequency (10^1 rad/s)			Frequency (10^2 rad/s)		
	G' (Pa $\times 10^2$)	G" (Pa $\times 10^4$)	G"/G'	G' (Pa $\times 10^4$)	G" (Pa $\times 10^4$)	G"/G'
PCL	8	1	1.25	2	5	2.5
PCL-CNT	20	1	0.5	2	5	2.5
PCL-o-CNT	8	0.002	0.025	2	0.02	0.01
PCL-HAp	8	1	1.25	2	5	2.5
PCL-o-CNT-HAp(1:2)	8	1	1.25	2	5	2.5
PLA	2	0.04	2.0	0.2	0.2	1.0
PLA-o-CNT-HAp(2:1)	2	0.04	2.0	0.2	0.2	1.0

4. Conclusion

The effect of low content (0.05 wt.%) of hybrid filler constituted of oxidized carbon nanotubes (o-CNT)/hydroxyapatite (HAp) at different proportions when added into PCL and PLA were evaluated. Infrared and X-ray diffraction evaluations did not show any variation for PCL and PLA materials. Molecular mobility by time domain nuclear magnetic resonance revealed signifcant variation in T_1 in the PLA-o-CNT-HAp(2:1) composite but for its counterpart PCL-o-CNT-HAp(1:2) T_2 remained quasi constant. These two composites also presented antagonistic behavior in TGA and DSC. Although both polymers are polyesters with distinct repeating units and the fillers also have uneven compositions which could indicate a limitation in the study, the hypotheses constructed regarding variations in properties and the possibility of interaction were supported by powerful techniques of characterization (TDNMR, DSC, and TGA). In summary, it was possible to suppose that difference of the chemical constitution of repeat unit of each polymer besides fillers' constitution and arrangement had an important role on the chemical interaction between polymer-filler and properties.

Conflicts of Interest

The authors declare no conflicts of interest regarding the publication of this paper.

References

[1] Walden, R., Jayadevan, S., Aliyana, A.K., Aazem, I., Perova, T., Hinder, S., *et al.* (2026) Effects of Pin-to-Plate Plasma on the TENG Properties of Electrospun PCL-Ag/PA6,6 Core-Sheath Yarns. *Materials Science and Engineering: B*, **327**, Article ID: 119258. https://doi.org/10.1016/j.mseb.2026.119258

[2] Mahović Poljaček, S., Tomašegović, T. and Priselac, D. (2026) Toward Sustainable Printed Packaging: Surface Properties and Ink Adhesion Behavior of PLA/PCL/Nanosilica Biopolymer Blends. *Polymers*, **18**, Article No. 422. https://doi.org/10.3390/polym18030422

[3] do Espirito Santo, G., Merlo, J.L., Botta, P., Rennó, A.C.M. and Rivero, G. (2025) Electrospun Polycaprolactone Scaffolds with Marine-Derived Biosilica Nanoparticles

(*Dragmacidon reticulatum*) for Bone Tissue Engineering Applications. *ACS Omega*, **10**, 56171-56182. https://doi.org/10.1021/acsomega.5c07836

[4] Hosseini, M., Najmoddin, N. and Zamanlouie, S. (2026) 3D Printed Biomimetic Nanocomposite Scaffold with Potential Osteo-Neurogenic Differentiation of Mesenchymal Stem Cells for Bone Repair. *Chemical Engineering Journal Advances*, **26**, Article ID: 101100. https://doi.org/10.1016/j.ceja.2026.101100

[5] Anitasari, S., Tandirogang, N., Irawiraman, H., Budi, H.S., Shen, Y., Alus, L.N., *et al.* (2026) Optimizing Graphene-Enhanced Polycaprolactone Scaffolds for Bone Tissue Engineering. *Journal of Oral Biology and Craniofacial Research*, **16**, Article ID: 101418. https://doi.org/10.1016/j.jobcr.2026.101418

[6] Kashanizadeh, P., Rad, I., hatamie, S. and Esmaeili, E. (2026) Biofunctional Electrospun PCL Scaffolds Incorporating Halloysite Nanoclay-Silver Nanohybrids for Antibacterial and Osteoinductive Bone Regeneration. *Polymer Bulletin*, **83**, Article No. 157. https://doi.org/10.1007/s00289-025-06246-9

[7] Pandey, R.P., Ouda, M., Almarzooqi, S.A., Almazrouei, R.M. and Hasan, S.W. (2026) Constructing Eco-Friendly, PLA/Silylpropyl Quaternary Ammonium Graphene Oxide Composite Membrane via Chemical Grafting for Improved Oil/Water Separation and Antibacterial Performance. *Cleaner Engineering and Technology*, **31**, Article ID: 101186. https://doi.org/10.1016/j.clet.2026.101186

[8] Yang, S., Li, J., Zhang, H., Guo, X., Dahanayake, R., Wang, Y., *et al.* (2026) Exceptional Mechanical Reinforcement of Polylactic Acid via 2D Conformal Coating of Graphene Oxide. *ACS Applied Materials & Interfaces*, **18**, 8908-8919. https://doi.org/10.1021/acsami.5c24140

[9] Sarosi, I., Paltinean, G.A., Moldovan, A., Cuc, S., Carpa, R., Sarosi, C., *et al.* (2026) Antimicrobial PLA-Based Composite Gels with Improved Functional Properties for Food Packaging. *Gels*, **12**, Article No. 194. https://doi.org/10.3390/gels12030194

[10] Dave, P.N., Macwan, P.M. and Kamaliya, B. (2024) Reinforcing Effect of Oxidized Multiwalled Carbon Nanotubes on Swelling and Mechanical Properties of Gum Ghatti-cl-poly(NIPAm-co-AA) Hydrogels. *Mechanics of Soft Materials*, **6**, Article No. 2. https://doi.org/10.1007/s42558-024-00057-0

[11] Lavagna, L., Bartoli, M., Suarez-Riera, D., Cagliero, D., Musso, S. and Pavese, M. (2022) Oxidation of Carbon Nanotubes for Improving the Mechanical and Electrical Properties of Oil-Well Cement-Based Composites. *ACS Applied Nano Materials*, **5**, 6671-6678. https://doi.org/10.1021/acsanm.2c00706

[12] Kim, Y.J., Shin, T.S., Choi, H.D., Kwon, J.H., Chung, Y. and Yoon, H.G. (2005) Electrical Conductivity of Chemically Modified Multiwalled Carbon Nanotube/Epoxy Composites. *Carbon*, **43**, 23-30. https://doi.org/10.1016/j.carbon.2004.08.015

[13] Zhou, X., Hu, A. and Zhou, J. (2026) Silver Nanoparticle-Decorated PCL Scaffolds: *In- Vitro* Antimicrobial Activity and Effects on Osteogenic Cell Responses. *Journal of Nanostructure in Chemistry*, **16**, 1-19.

[14] Faramarzi Jolfaei, A. and Haddadi-Asl, V. (2026) Enhanced PCL Bimodal Foams Utilizing Phospho-Calcified Graphene Oxide to Promote Osteogenic Differentiation of HMSCs. *Colloid and Interface Science Communications*, **72**, Article ID: 100883. https://doi.org/10.1016/j.colcom.2026.100883

[15] Fallah, R., Zahedi, P., Shams, S., Nazari, A., Naderi, F., Khosroabadi, K., *et al.* (2026) Poly(ε-Caprolactone)/Poly(ethylene Oxide)/Hydroxyapatite Nanofibrous Composite Scaffolds Used for Bone Tissue Regeneration, Potentially: Effect of Chamomile Extract. *Materials & Design*, **265**, Article ID: 115827. https://doi.org/10.1016/j.matdes.2026.115827

[16] Jiang, H., Fu, H., Wei, Q. and Wang, Y. (2026) A Hierarchical Bilayer Sponge Dressing Based on QCMCS@GO/PLA for Synergistic Wound Healing via Hemostasis and Anti-Adhesion. *International Journal of Biological Macromolecules*, **344**, Article ID: 150565. https://doi.org/10.1016/j.ijbiomac.2026.150565

[17] Keerthi, A.S., Manju, M.S., Thomas, L.V. and Sujith, A. (2026) Design of Thermoplastic and Few-Layer Graphene Modified Epoxy Coatings with Semi-Interpenetrating Polymer Networks for Hydrogen-Bond Mediated Self-healing and Mechanical Performance Enhancement. *Journal of Applied Polymer Science*, **143**, e70617. https://doi.org/10.1002/app.70617

[18] Litha, T.T., Nair, P.P. and Sajith Babu, C. (2026) A Novel Dual Nano-Filler Reinforcement System (Graphene Oxide-Hydroxyapatite/cellulose Nano-Whiskers) of PLA/PCL Bio-Nanocomposites for Enhanced Biomechanical Properties. *The European Physical Journal Special Topics*. https://doi.org/10.1140/epjs/s11734-026-02236-8

[19] Pekdemir, M.E., Kök, M., Qader, I.N. and Aydoğdu, Y. (2022) Preparation and Physicochemical Properties of MWCNT Doped Polyvinyl Chloride/Poly(ε-Caprolactone) Blend. *Journal of Polymer Research*, **29**, Article No. 109. https://doi.org/10.1007/s10965-022-02947-1

[20] Qader, I.N., Kök, M., Mohammed, K.S., Coskun, M., Öner, E.Ö. and Aydoğdu, Y. (2025) Development of a PLA/PHA-TiO_2 Polymer Blend with Improved Physicochemical and Thermal Properties. *Journal of Polymers and the Environment*, **33**, 2502-2514. https://doi.org/10.1007/s10924-025-03547-y

[21] Demir, P. (2023) Thermal Degradation Kinetics, Mechanism, Thermodynamics, Shape Memory Properties and Artificial Neural Network Application Study of Polycaprolactone (PCL)/Polyvinyl Chloride (PVC) Blends. *Polymer Bulletin*, **80**, 9685-9708. https://doi.org/10.1007/s00289-022-04522-6

[22] Abdelrazek, E.M., Hezma, A.M., El-Khodary, A., Elzayat, A.M. and Rajeh, A. (2023) Modifying of Structural, Optical, Thermal, and Mechanical Properties of PCL/PMMA Biomaterial Blend Doped with MWCNTs as an Application in Materials Science. *Journal of Inorganic and Organometallic Polymers and Materials*, **33**, 4117-4126. https://doi.org/10.1007/s10904-023-02625-9

[23] Mantecón-Oria, M., Tapia, O., Lafarga, M., Berciano, M.T., Munuera, J.M., Villar-Rodil, S., *et al.* (2022) Influence of the Properties of Different Graphene-Based Nanomaterials Dispersed in Polycaprolactone Membranes on Astrocytic Differentiation. *Scientific Reports*, **12**, Article No. 13408. https://doi.org/10.1038/s41598-022-17697-9

[24] Pereira, K.A.B., Cestari, S.P., Cucinelli Neto, R.P., Macedo, K.R.M. and Mendes, L.C. (2019) Oxidized-Sulfonated Multi-Walled Carbon Nanotube/Hydroxyapatite Hybrid Particles: Synthesis and Characterization. *Journal of Solid State Chemistry*, **279**, Article ID: 120924. https://doi.org/10.1016/j.jssc.2019.120924

[25] Contreras, M.M., Nascimento, C.R., Cucinelli Neto, R.P., Teixeira, S., Berry, N., Costa, M.F., *et al.* (2018) TD-NMR Analysis of Structural Evolution in PVDF Induced by Stress Relaxation. *Polymer Testing*, **68**, 153-159. https://doi.org/10.1016/j.polymertesting.2018.03.051

[26] Ramos, V.S., Merat, P.P., Iulianelli, G., Silva, E.M., Bello, T.M.H. and Tavares, M.I.B. (2023) Extraction of Stem Oils from Cinnamomum Cassia and NMR Characterization to Produce Nutraceuticals. *Food Science and Technology*, **43**, e14523. https://doi.org/10.5327/fst.14523

[27] Fernández-Tena, A., Pérez-Camargo, R.A., Coulembier, O., Sangroniz, L., Aranburu,

N., Guerrica-Echevarria, G., *et al.* (2023) Effect of Molecular Weight on the Crystallization and Melt Memory of Poly(ε-Caprolactone) (PCL). *Macromolecules*, **56**, 4602-4620. https://doi.org/10.1021/acs.macromol.3c00234

[28] Akdevelioğlu, Y., Alanalp, M.B., Randall, J., Gehrung, M., Durmus, A., Jahani, D., *et al.* (2026) Joncryl Chain Extender Reactivity with Polylactide: Effect of PLA Molecular Weight and the Resultant Rheological and Crystallization Behaviors. *Journal of Polymers and the Environment*, **34**, Article No. 21. https://doi.org/10.1007/s10924-025-03753-8

[29] Adeniyi, M., Parvin, M., Akter, K., Arbab, A.S., Quirino, R.L. and Khan, M. (2026) Synthesis and Processing of PCL (Polycaprolactone) and IRDye Nanoparticles and Their Biodistribution. *BioMedical Engineering OnLine*, **25**, Article No. 49. https://doi.org/10.1186/s12938-026-01544-3

[30] Justino Netto, J.M., Sousa, D., Amaral, P. and Leite, M. (2026) Feedstock Characterization and Process Calibration for Fused Pellet Fabrication of PLA/Limestone Composites. *Progress in Additive Manufacturing*, **11**, 4061-4075. https://doi.org/10.1007/s40964-026-01567-1

[31] Ramírez-Pedroza, J.P., del Pilar Ramos-Godínez, M., Ali, A., Tomás-Velázquez, S.A., Hernández-Martínez, E. and Luna-Arias, J.P. (2026) Hydroxyapatite Nanoparticles Synthesis with PAMAM-Like Dendrimers Grown in Situ on Their Surface for Potential Therapeutic Use. *Journal of Nanoparticle Research*, **28**, Article No. 99. https://doi.org/10.1007/s11051-026-06626-w

[32] Targońska, S., Kardach, M., Andrzejewski, J., Wiatrak, B., Nowotarska, P., Gębarowski, T., *et al.* (2026) Effect of Carbon Fibers Coated with Nanosized Hydroxyapatite on the Strength and Biocompatibility of Polymer Composites. *Journal of Applied Polymer Science*, **143**, e58139. https://doi.org/10.1002/app.58139

[33] Cao, L., Zhang, J., Chen, S., Osaka, A. and Chen, W. (2026) Fabrication, Characterization, Tailored Structure, and *in Vitro* Biocompatibility of Hydroxyapatite Hollow Microspheres. *International Journal of Applied Ceramic Technology*, **23**, e70143. https://doi.org/10.1111/ijac.70143

[34] Puliyasseri, R., Haribabu, J., Arulraj, A., Moraga, D., Nishanth, T. and Sastikumar, D. (2026) Boron-Doped Graphene Oxide Nanoparticles Synthesized by Nanosecond Pulsed Laser Ablation of Graphene in Ethanol: Structural, Optical, and Bioimaging Studies. *Optics & Laser Technology*, **194**, Article ID: 114371. https://doi.org/10.1016/j.optlastec.2025.114371

[35] Saipanya, S., Sriwichai, S., Themsirimongkon, S., Sudrungruang, S., Jakmunee, J. and Waenkaew, P. (2026) Electrodeposition of Platinum on Electropolymerized Poly(3-Aminobenzylamine)-Graphene Oxide as a Catalyst for Alcohol Oxidation in Alkaline Solution. *International Journal of Hydrogen Energy*, **206**, Article ID: 153444. https://doi.org/10.1016/j.ijhydene.2026.153444

[36] Doostmohammadi, N., Yousefpour, M., Nourbakhsh, M.S. and Bahraminasab, M. (2025) Fabrication and Characterization of 3D Printed PCL/ZrO_2/FA Scaffolds for Bone Tissue Engineering. *Materials Chemistry and Physics*, **338**, Article ID: 130659. https://doi.org/10.1016/j.matchemphys.2025.130659

[37] Tamburini, G., Bertagnoli, S., Tarricone, G., Piva, S., Sassella, A., Lorenzi, R., *et al.* (2023) Early Stages of X-Ray Induced Molecular Unit Modifications in Poly(lactic acid). *Polymer Degradation and Stability*, **216**, Article ID: 110485. https://doi.org/10.1016/j.polymdegradstab.2023.110485

[38] Nurbaiti,, Herliansyah, M.K., Tontowi, A.E., Widiastuti, M.G., Hoten, H.V. and Perkasa, D.P. (2025) Characterization of Three-Dimensional Printed Hydroxyap-

atite/collagen Composite Slurry. *Materials Chemistry and Physics*, **329**, Article ID: 130047. https://doi.org/10.1016/j.matchemphys.2024.130047

[39] Gómez, S., Rendtorff, N.M., Aglietti, E.F., Sakka, Y. and Suárez, G. (2016) Surface Modification of Multiwall Carbon Nanotubes by Sulfonitric Treatment. *Applied Surface Science*, **379**, 264-269. https://doi.org/10.1016/j.apsusc.2016.04.065

[40] Irani, M., Nasirtabrizi, M.H., Ezzatzadeh, E. and Sadeghianmaryan, A. (2025) *In-Vitro* Study of Co-Electrospun PCL/Gelatin/Chitosan Scaffolds Enhanced with Carbon Nanotube for Cartilage Regeneration. *Polymer Bulletin*, **82**, 6981-6999. https://doi.org/10.1007/s00289-025-05808-1

[41] Catauro, M., Bollino, F., Cristina Mozzati, M., Ferrara, C. and Mustarelli, P. (2013) Structure and Magnetic Properties of SiO_2/PCL Novel Sol-Gel Organic-Inorganic Hybrid Materials. *Journal of Solid State Chemistry*, **203**, 92-99. https://doi.org/10.1016/j.jssc.2013.04.014

[42] Çelik, R.H., Şimşek, S., Gel, E. and Acuner, S.E. (2025) Molecular Dynamics Insights into the Interactions of Biocompatible Synthetic Polymer Composites with Carbon-Based Nanoparticle Derivatives: A Comparative Study of PLGA and PCL Interactions with GO/rGO. *Journal of Computer-Aided Molecular Design*, **40**, Article No. 19. https://doi.org/10.1007/s10822-025-00726-w

[43] Mohammed, K.S., Coskun, M., Babakr, K.A., Kök, M. and Qader, I.N. (2025) Blending of Polycaprolactone with Polyvinyl Chloride Polymers Using Silica Gel as a Functional Reinforcement. *Journal of Materials Science: Materials in Electronics*, **36**, Article No. 2020. https://doi.org/10.1007/s10854-025-16102-1

[44] Mahović Poljaček, S., Priselac, D., Tomašegović, T., Elesini, U.S., Leskovšek, M. and Leskovac, M. (2022) Effect of the Addition of Nano-Silica and Poly(ε-Caprolactone) on the Mechanical and Thermal Properties of Poly(lactic acid) Blends and Possible Application in Embossing Process. *Polymers*, **14**, Article No. 4861. https://doi.org/10.3390/polym14224861

[45] Taha, E.O., Shoaib, E., Ahmed, M.A., El-Ghazawy, R.A. and Naguib, H.M. (2026) Smart Biodegradable PLA Nanocomposites Reinforced with ZnO and GO for Thermomechanical and Shape Memory Applications. *Discover Materials*, **6**, Article No. 131. https://doi.org/10.1007/s43939-026-00623-5

[46] Oliver-Cuenca, V., Salaris, V., Muñoz-Gimena, P.F., Agüero, Á., Peltzer, M.A., Montero, V.A., *et al.* (2024) Bio-Based and Biodegradable Polymeric Materials for a Circular Economy. *Polymers*, **16**, Article No. 3015. https://doi.org/10.3390/polym16213015

[47] Lomakin, S., Koverzanova, E., Usachev, S., Shilkina, N., Khvatov, A., Erina, N., *et al.* (2026) Specific Impact of the Layered Nanomodifiers—Graphene Nanoplates, and Na^+ Montmorillonite on Thermal Degradation of Polylactic Acid: Mechanism and Kinetics. *Polymers*, **18**, Article No. 347. https://doi.org/10.3390/polym18030347